Mechanism study of self-organized TiO_2 nanotube arrays by anodization

Jinliang Tao, Jianling Zhao, Chengcun Tang, Yingru Kang and Yangxian Li*

Received (in Gainesville, FL, USA) 23rd May 2008, Accepted 20th June 2008
First published as an Advance Article on the web 1st September 2008
DOI: 10.1039/b808719a

Based on analysis of the current–time curve and observation of surface morphology including top, cross-section, bottom and substrate views by scanning electron microscopy (SEM), a new growth, dissolution–breakdown model, of self-organized titania nanotube arrays is presented. By this model, many phenomena raised during anodization are explained, such as the sharp decrease of current in initial period, current transient, occurring of ridges on tube walls, and formation of not pores but tubes *etc*. Furthermore, the reason for the occurrence of a porous structure, the balance between internal energy and surface energy, was proposed too. This study may also shed light on the formation of porous oxide films on other valve metals.

Introduction

Over the past few years, the formation of high surface TiO_2 nanotubes has attracted much attention due to their wider applications in sensing devices,[1] photocatalysis,[2] tissue engineering[3] and solar cells[4] *etc*. Using different synthesis routes, such as sol–gel,[5] template synthesis,[6,7] hydrothermal processes,[8–10] and anodization,[11] TiO_2 nanotubes have been formed successfully. Among these methods, electrochemical anodization has attracted many researchers' interest due to its lower cost, large area fabrication and ordered arrangement. Moreover, the nanotubes formed by anodization have good mechanical adhesion and electrical conductivity due to their special structure in which nanotubes connect directly to the substrate. Most importantly, the parameters of these nanotubes, such as the inner diameter, wall thickness and length, can be controlled easily by adjusting the electrochemical conditions, for example, anode voltage, oxidized time, and compositions of electrolyte *etc*. However, due to the complexity of the electrochemical reaction, the cognition to the fabrication process of nanotubes has never stopped from the beginning, *i.e*. the first report of titania nanotube arrays with a length of about 250 nm in an aqueous HF-based electrolyte in 2001,[12] to the formation of nanotube arrays up to 1 mm long using an organic electrolyte in 2007.[13]

Up to now, many different morphologies and structures of nanotubes, such as conical-shaped,[14] smooth,[15] Y-branched[16] multiple layers[17] and self-standing[18] have been fabricated successfully. Furthermore, the formation mechanism of nanotube arrays was also mentioned briefly,[14,19–22] in which the key processes of nanotube growth were described as: (1) oxide growth at the surface of the metal occurs due to interaction of the metal with O^{2-} or OH^- ions. (2) Metal ions (Ti^{4+}) migration from metal at the metal–oxide (MO) interface; Ti^{4+} cations will be ejected from the metal–oxide interface under application of an electric field and move towards the oxide–electrolyte (OE) interface. (3) Field-assisted dissolution of the oxide at OE interface. (4) Chemical dissolution of the metal, or oxide, by the acidic electrolyte also takes place during anodization. However, both as valve metals, the oxide morphology of titanium is very different from that of aluminium, although the key processes responsible for anodic formation of tubular titania and porous alumina are thought to be same.[22] Therefore, a more comprehensive and detailed formation mechanism of nanotube arrays need to be proposed. In this work, based on analysis of the current–time curve and observation of nanotubes morphology, a new growth, dissolution–breakdown model was put forward. The new model explains many phenomena occurred during anodiztion well and may shed light on the formation of porous oxide films on other valve metals.

School of Material Science and Engineering, Hebei University of Technology, Tianjin 300130, China. E-mail: hebutzhaoj@126.com; Fax: +86 22 60202214; Tel: +86 22 60202214

Experimental foundation

1 SEM images of nanotube arrays

Fig. 1. shows the typical morphology of titania nanotube arrays formed by electrochemical anodization. According to these SEM images, some characteristics of this structure can be described as the following. First, the structure is tubular. Each pore has its own wall and is separated from others by interspace, which is very different from alumina nanopores. Second, the tube mouths are open while their ends are closed. Third, the nanotubes are all well-ordered and perpendicular to the Ti substrate. Fourth, there exist some ridges on the tube wall. Finally, the oxide–metal interface (OM) is not planar. Many convex and concave arrangements can be observed clearly on the barrier layer as well as the Ti substrate. Herein, the images of different anodic time are not given and can be observed in ref. 14 and 19.

2 Current–time curve

Essentially, anodization is a chemical process accompanying electron transfer. Therefore, it can be reflected well by variation of electric current.

Fig. 2a exhibits a typical current–time curve during anodization. It obviously goes through four stages: an abrupt decrease in the initial step (before P_1), a sudden increase at

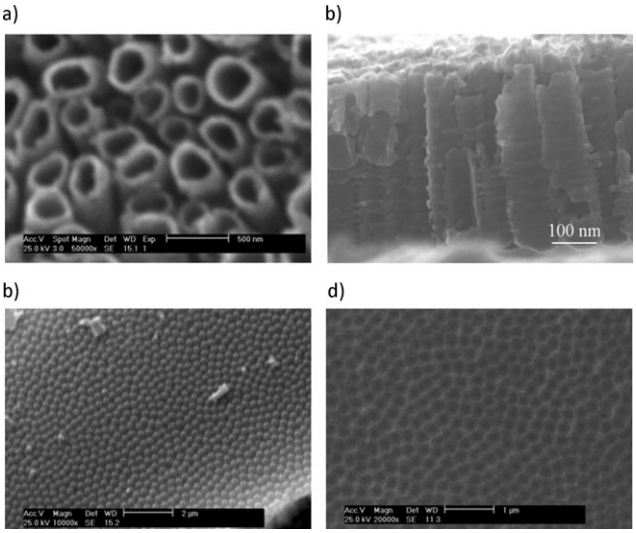

Fig. 1 Images of titania nanotube arrays. (a–c) are top, cross-section and bottom SEM images of titania nanotube arrays, respectively, and (d) is the Ti substrate.

75–160 s (P_1–P_2), then a slowly decrease at 160–600 s (P_2–P_3), and finally keep steady (after P_3). However, as shown in Fig. 2b, the decreasing trend after P_0 is different from that before P_0 in which ln(I) and t have a good linear relationship. In addition, current oscillations can be observed clearly from the inset image of Fig. 2b.

Formation mechanism of nanotube arrays

1 Mechanistic model of nanotube array formation

As shown in Fig. 3, the growth process of nanotubes is sketched out by ten steps.

In this model, the following assumptions are made:

(1) The field intensity inside the oxide layer will decrease quickly with increasing distance due to the higher dielectric constants of titania.

(2) The barrier layer is thin enough for iron migration under electric field.

(3) In the process of anodization, the main energy barriers to cation and anion migration exist at the MO and OE interfaces, respectively. Once the ion is within barrier layer, transfer is rapid due to the high applied field.

2 Growth mechanism of nanotube arrays

According to current curves, the growth process of nanotubes can be described as:

(1) establishment of bilayer-film (before P_0 and corresponding with step 1–2). With the onset of anodization, selective oxidation takes place due to the electric field and higher energy on the partial area of the titanium surface. As a result, some tiny titania clusters arise on the substrate here and there (step 1). Then around these cores, the clusters develop in all directions and finally connect with each other. This process happens very quickly and can be described as:

$$2H_2O - 4e^- \rightarrow O_2 + 4H^+$$
$$Ti + O_2 \rightarrow TiO_2 \qquad (1)$$

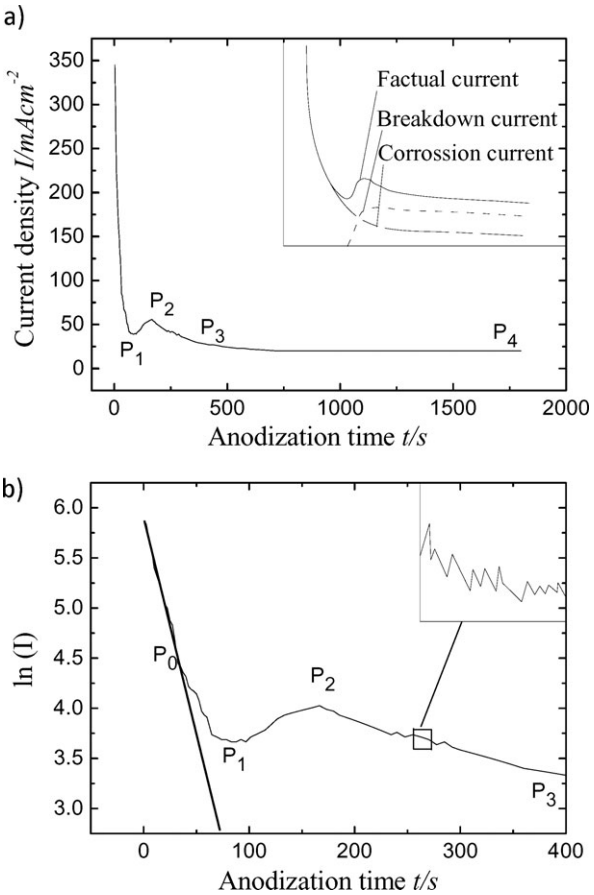

Fig. 2 Current density (I)–time (t) curves. (a) is I–t response; the inset is an exploded view of electric current. (b) ln(I)–t response, the inset is a closer look at current oscillations.

From the higher electric current at the beginning of the experiment, we can conclude that the layer is thin enough and O_2 can transfer through it easily and react with the inner metal. With ongoing reaction, however, a compact layer forms due to the volume expansion (step 2). We know that the bond lengths of Ti–Ti and Ti–O are 0.189 nm and 0.185 nm, respectively. Obviously, with the generation of TiO_2, the volume must expand in some degree due to the participation of O atoms. The expansion coefficient (η) can be calculated using the following formula:

$$\eta = \frac{Md}{nAD} \approx \frac{89.87 \times 4.5}{1 \times 47.87 \times 4} = 2.11 \qquad (2)$$

where M is molecular weight of titania, A is atomic weight of titanium, d is density of titanium, D is density of titania and n is the number of titanium atoms in titania.

Therefore, we have reason to believe that there must be volume stresses in the subsequent forming layer because of volume expansion.

(2) Formation and development of corrosion pits (P_0–P_1 and corresponding with step 3–6). With the increase in the compact film thickness, the volume stress becomes higher and higher. At the same time, it becomes more difficult for the reaction heat to get out. It has been reported that the heat of reaction is one of the other key factors in the formation of

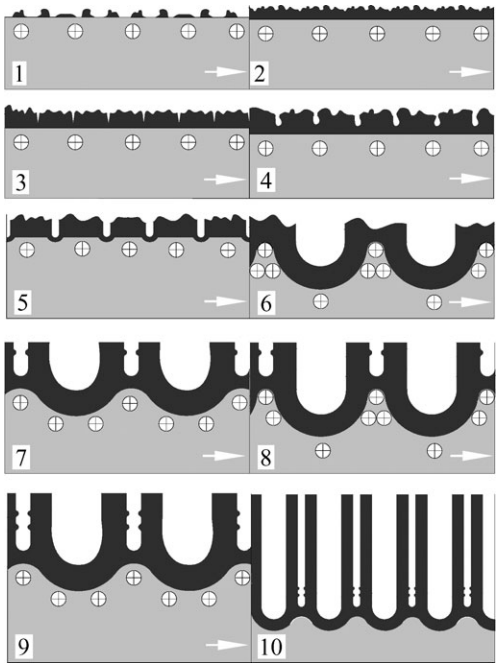

Fig. 3 Schematic diagrams illustrating formation of titania nanotube arrays. (1) Creation of loose layer; (2) establishment of compact layer; (3) occurrence of microcracks; (4) developing of microcracks; (5) formation of corrosion pits; (6) expansion of corrosion pits; (7) breakdown of interpores; (8) chemical dissolution of inner pores; (9) breakdown of interpores again; (10) well-ordered nanotubes arrays.

oxide film for valve metal, as well as the volume expansion coefficient.[23] Whether volume expansion or reaction heat (for titania, it is about 944 KJ mol^{-1}), they all make the internal energy increase. In order to lower them, the surface energy must increase. So a large number of microcracks arise, as shown in step 3. In the growth process of nanotubes arrays, as it were, cracks play an important role on the morphology because they are the foundation of corrosion pit formation. Due to the occurrence of microcracks, the electric field distribution within oxide film changes, especially, the field at the tip of the cracks increase greatly. As a result, the concentrations of anions, such as F^- and O^{2-}, also increase because of electrostatic attraction. Furthermore, the Ti–O bond becomes weakened due to polarization by higher electric field.[3] So compared with the surface of the titania, it makes it easier for Ti^{4+} ions to dissolve in the electrolyte. This reaction of chemical dissolution can be described as below:

$$6F^- + TiO_2 + 4H^+ \rightarrow [TiF_6]^{2-} + 2H_2O \qquad (3)$$

In conclusion, due to the acceleration of the localized dissolution rate in cracks, microcells originate in this compact oxide layer (step 4). Those cells having a relatively thin barrier layer at the bottom, on the one hand, increase the electric field intensity across the remaining barrier layer, resulting in further cell expansion; and on the other hand, provide an easier pathway for more anions to migrate through the barrier layer, leading to further metal oxidization. So corrosion pits occur beneath those cells (step 5) and grow upwards with time, which leads to a difference of charge distribution between convex and concave (step 6). At this stage, the tendency of the current decrease to slow down may result from the formation of corrosion pits (P_0–P_1 in Fig. 2b).

(3) Breakdown of interpores and formation of tubes (P_1–P_2 and corresponding with step 7)

In the process of anodization, the main energy barrier (W) to Ti^{4+} migration exists at the MO interface, as shown in Fig. 4. Under the applied field, W is lowered by an amount equal to:[23]

$$W - qa\frac{V}{x} \qquad (4)$$

where V is potential, x is the thickness of oxide film, a is the distance between two adjacent lattice sites, and q is the charge of the metal ions.

In step (6), the curvature radius of the residual metal among cells will become smaller and smaller because of the chemical dissolution occurring in downward semi-sphere cells, which leads to an increasing of local potential. When $qaV/x = W$, the energy barrier at the MO interface turns to zero, that is, Ti^{4+} ions can leave the metal surface and puncture the barrier layer above itself easily. As a result, the interspaces or the tubular structure comes into being. As traces of breakdown, some ringed ridges are left on the tube wall, as shown in Fig. 1b.

(4) Growth of nanotubes (P_2–P_3 and corresponding with step 8–10). The growth of nanotubes is a process of alternative proceeding between chemical dissolution of inner tube and breakdown of interpores, where the chemical dissolution is continuous and the breakdown is intermittent. It is the intermittency of breakdown that leads to current transient.

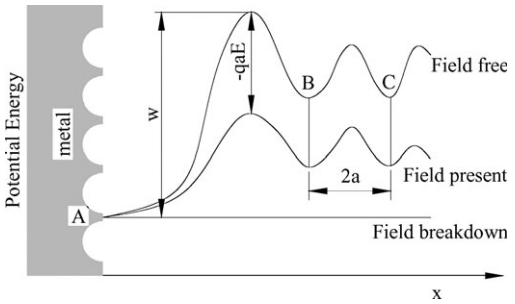

Fig. 4 Potential energy diagram. A is the ion at rest at the MO interface; W is energy that occurs when an ion moves from the surface into the bulk; $2a$ is the distance between two adjacent lattice sites, B and C; x is the thickness of the oxide film; V is applied local potential; q is the charge of the metal ions.

3 Analysis of phenomena

(1) Formation of tubular structure. The occurrence of porous structure is an inevitable result of the balance between internal energy and surface energy. Only those metals that had bigger volume expansion coefficients and higher reaction heats when anodized to their oxides can form the porous structure. However, the morphology of titania is tubular and very different from alumina, which is porous. This difference may be related to their dielectric constants: they are 9.77 and about 100 for alumina and titania powders, respectively. According to assumption (1) of this model, the field intensity inside the oxide layer will decrease greatly with increasing distance. For

titania, the higher dielectric constants restrict the transfer of ions. So some unoxidized residual metal is left and ultimately forms interspace by breakdown.

(2) Current variation during anodization. Since the anodic oxidation is composed of two different reactions, its current can be broken into two parts. One is dissolution current and the other is breakdown current, as shown in the inset of Fig. 2. In the initial stage, the current is provided only by dissolution reaction. The growth rate of the film depends strongly on the transfer rates of ions crossing the compact layer. As can be seen from Fig. 2b (before P_0), $\ln(I)$ and t have a linear relationship. This can be described as:

$$\ln(I) = -kt \text{ or } I = e^{-kt} \quad (5)$$

So a sharp, exponential decrease of current is observed. Then the occurrence of corrosion pits slow its decreasing rates (P_0–P_1) till the breakdown happens. Accordingly, the current increases suddenly and relatively regular current oscillations that correspond to breakdowns or ridges on the tube wall are observed (P_1–P_2). When the breakdown is fully developed, the current reaches its maximum (P_2). After P_2, the current decreases slowly due to the tube growth and finally remains steady.

(3) Process of chemical reaction. During the anodization of the metal, two compounds of titanium are produced: one is TiO_2 and the other is TiF_6^{2-}. So the whole reaction could be written as:

$$(n+1)\mathrm{Ti} + 2n\mathrm{H_2O} + 6\mathrm{F^-} \rightarrow 4(n+1)\mathrm{e^-} + 4n\mathrm{H^+} + n\mathrm{TiO_2} + \mathrm{TiF_6^{2-}} \quad (6)$$

where n is molar ratio between TiO_2 and TiF_6^{2-}.

Note that TiF_6^{2-} results from the dissolution of TiO_2 in nanopores (eqn (3)). So n also can be defined as the cross-section area (CSA) ratio between wall and interpore approximately, as shown in eqn (7).

$$n = \frac{\mathrm{mol_{TiO_2}}}{\mathrm{mol_{TiF_6^{2-}}}} \approx \frac{\mathrm{CSA_{wall}}}{\mathrm{CSA_{pore}}} \quad (7)$$

Herein, the value of n may be related to the reaction temperature and anodic potential. From eqn (6), it can be obtained that 4 mol H^+ produce an accompanying 1 mol TiO_2. So we may draw a conclusion that a local acidic electrolyte at the bottom of the tube is necessary for the chemical reaction even though a neutral electrolyte is chosen.

(4) Process of self-organization. The formation of nanotube arrays is a self-organized process. First, the occurrence of nanopores is the result of the balance between internal energy and surface energy. For one single pore, its surface energy is directly proportional to its diameter. In order to achieve homogeneous distribution of system energy, the pores diameter will be self-regulated and tend to form an ordered nanotube array with maximal packing density. Second, the growth of pores is related to the formation of the oxide film at MO interface and dissolution of oxide film at OE interface of pore bottom. There exists a stable equilibrium between the two reactions above. During the period of nanotube growth (stage 4) the thickness of the barrier layer is adjusted automatically. When it becomes thinner, the electrical field strength at the OE interface will increase drastically, which results in increasing migration rate of oxygen ions through the barrier layer, making itself thicker. And the reverse is true as well.

Conclusions

In this paper, a new growth, dissolution–breakdown model, of titania nanotubes is presented, in which the key processes can be described as: (1) establishment of bilayer-film; (2) formation and development of corrosion pits; (3) breakdown of interpores and formation of tubes; and 4) growth of nanotubes. Based on this model, four conclusions were made:

(1) The occurring of porous structure is a result of the balance between internal energy and surface energy. Moreover, the occurring of not pores but tubes may result from the higher dielectric constants of titania.

(2) The current variation is affected by both dissolution and breakdown.

(3) The local acidic environment at the bottom of nanotubes is necessary for chemical dissolution of oxide at the OE interface.

(4) The growth of nanotubes is a self-organized process. The diameter and growth rate of nanotube will be auto-adjusted because of the dynamic balance between internal and surface energy and the balance between forming of oxide film at MO interface and dissolution of oxide film at OE interface of pore bottom, respectively.

Acknowledgements

This work is supported by Tianjin Natural Science Foundation (07JCYBJC03300) and Natural Science Foundation of Hebei Province of China (E2007000044).

References

1 M. Paulose, O. K. Varghese, G. K. Mor and C. A. Grimes, *Nanotechnology*, 2006, **17**, 398.
2 J. M. Macak, H. Tsuchiya, S. Bauer, A. Ghicov, P. Schmuki, P. J. Barczuk, M. Z. Nowakowska, M. Chojak and P. J. Kulesza, *Electrochem. Commun.*, 2005, **7**, 1417.
3 J. M. Macak, H. Tsuchiya, L. Taveria, A. Ghicov and P. Schmuki, *J. Biomed. Mater. Res. A*, 2005, **75**, 928.
4 G. K. Mor, K. Shankar, M. Paulose, O. K. Varghese and C. A. Grimes, *Nano Lett.*, 2006, **6**, 215.
5 J. H. Jung, H. Kobayashi, K. J. C. van Bommel, S. Shinkai and T. Shimizu, *Chem. Mater.*, 2002, **14**, 1445.
6 D. G. Shchuki and R. A. Caruso, *Adv. Funct. Mater.*, 2003, **13**, 789.
7 S. M. Liu, L. M. Gan, L. H. Liu, W. D. Zhang and H. C. Zeng, *Chem. Mater.*, 2002, **14**, 1391.
8 M. A. Khan, H.-T. Jung and B. Yang, *J. Phys. Chem. B*, 2006, **110**, 6626.
9 D. V. Bavykin, V. N. Parmon, A. A. Lapkina and F. C. Walshc, *J. Mater. Chem.*, 2004, **14**, 3370.
10 Y. Lan, X. Gao, H. Zhu, Z. Zheng, T. Yan, F. Wu, S. P. Ringer and D. Song, *Adv. Funct. Mater.*, 2005, **15**, 1310.
11 A. Nakahira, K. Konishi, K. Yokota, T. Honma, H. Aritani and K. Tanaka, *J. Ceram. Soc. Jpn.*, 2006, **114**, 46.
12 D. Gong, C. A. Grimes and O. K. Varghese, *J. Mater. Res.*, 2001, **16**, 3331.

13 M. Paulose, H. E. Prakasam, O. K. Varghese, L. Peng, K. C. Popat, G. K. Mor, T. A. Desai and C. A. Grimes, *J. Phys. Chem. C*, 2007, **111**, 14992.
14 G. K. Mor, O. K. Varghese, M. Paulose, N. Mukherjee and C. A. Grimes, *J. Mater. Res.*, 2003, **18**, 2588.
15 J. M. Macak, H. Tsuchiya, L. Taveira, S. Aldabergenova and P. Schmuki, *Angew. Chem., Int. Ed.*, 2005, **44**, 7463.
16 S. K. Mohapatra, M. Misra, V. K. Mahajan and K. S. Raja, *Mater. Lett.*, 2008, **62**, 1772.
17 J. M. Macak, S. Albu, D. H. Kim, I. Paramasivam, S. Aldabergerova and P. Schmuki, *Electrochem. Solid State Lett.*, 2007, **10K**, 28.
18 H. E. Prakasam, K. Shankar, M. Paulose, O. K. Varghese and C. A. Grimes, *J. Phys. Chem. C*, 2007, **111**, 7235.
19 S. H. Kang, J. Y. Kim, H. S. Kim and Y. E. Sung, *J. Ind. Eng. Chem.*, 2008, **14**, 52.
20 J. L. Zhao, X. X. Wang, R. Chen and L. Li, *Solid State Commun.*, 2005, **134**, 705.
21 Craig A. Grimes, *J. Mater. Chem.*, 2007, **17**, 1451.
22 G. K. Mor, O. K. Varghese, M. Paulose, K. Shankar and C. A. Grimes, *Sol. Energy Mater. Sol. Cells*, 2006, **90**, 2011.
23 M. N. Denise, *PhD Thesis*, Texas A&M University, 1994.

